14th International Congress on Civil Engineering, 21-23 October 2025
Sharif University of Technology, Tehran, Iran

Finite Element Assessment of Multi-Tierd Eccentrically Braced Frames under Seismic Loading with Shear Link

Mohammad Rezaee[1], Abazar Asghari[2]

1- M.Sc. Student, School of Civil Engineering, College of Engineering, University of Tehran, Tehran, Iran.

2- Associate Professor, School of Civil Engineering, College of Engineering, University of Tehran, Tehran,

Abazar.asghari@ut.ac.ir

Abstract

Multi-tiered eccentrically braced frames (MT-EBF) are a modified version of eccentrically braced frames (EBF), where each story is divided into multiple tiers of braces accompanied by a split link. This system is typically used as a lateral load-resisting system in high-rise structures within a single story. In this study, the behavior of two MT-EBF frames with I-shaped and Box link was evaluated across four intermediate tiers. Since seismic design requirements for this system are not explicitly addressed in any seismic codes, the system was initially assessed in accordance with the AISC 341-22 provisions, similar to the seismic regulations for conventional EBF. This study investigates whether the new structural system can be designed in accordance with the current seismic provisions of the code. The nonlinear behavior of the system was analyzed using the Abaqus finite element software, focusing on the lateral-torsional buckling of intermediate-tier beams and column buckling. The seismic performance evaluation revealed that I-shaped link, connected to the beam via gusset plates, experienced lateral buckling in intermediate-tier beams lacking lateral bracing. In contrast, Box link did not exhibit lateral buckling. However, the first-tier columns under axial compressive forces demonstrated buckling behavior and failed to exhibit stable performance.

Keywords: Multi-Tired Eccentrically Braced Frame, Eccentrically Braced Frame Braced Frame, Seismic Analysis, Nonlinear Analysis, Abaqus

1- INTRODUCTION

Multi-tiered eccentrically braced frames (MT-EBFs) are a combination of conventional eccentrically braced frames (EBFs) [1] and multi-tiered braced frames (MTBFs) [2]. MTBFs are typically utilized as lateral-force-resisting systems in structures with large inter-story heights. These frames differ from conventional braced frames in two primary ways: (1) the absence of diaphragms between tier levels, spanning from roof to foundation, and (2) the lack of lateral bracing for intermediate beams and columns. MTBFs are particularly suitable for tall, open structures where the use of long continuous braces often leads to impractical or uneconomical design solutions [3].

MT-EBFs are increasingly employed as lateral load-resisting systems, particularly in high seismic hazard regions, due to their superior ductility, stable and reliable yielding mechanism, and architectural flexibility when compared to multi-tiered concentrically braced frames (MT-CBFs). The EBF system itself is a hybrid of concentrically braced frames and moment-resisting frames. It provides high elastic stiffness while developing significant inelastic responses during seismic events [4]. The primary energy-dissipating element in such systems is the link, while the remaining structural components are expected to remain elastic under lateral seismic loading. The behavior of the link beam may be governed by shear, flexural-shear, or flexural mechanisms, depending on the ratio of its plastic moment and shear capacities to its length. The various configurations of MTBFs are illustrated in Figure 1.

(a) **(b)** **(c)**

Figure 1- The various configurations of multi-tier braced frames (a) multi-tiered concentrically braced frames (MT-CBF) (b) multi-tiered eccentrically braced frames (MT-EBF) (c) multi-tiered buckling-restrained braced frames (MT-BRBF) [5]

Initial research on multi-tiered braced frames focused on MT-CBFs [6]. Numerical evaluation of a four-tier concentrically braced frame designed per AISC 2010 seismic provisions revealed vulnerability to inelastic drift concentration at a specific bracing tier, along with substantial in-plane flexural demands on columns. The study indicated that flexural yielding in columns may jeopardize overall stability, and that higher ductility demands arise at tiers where deformation localizes [7]. Subsequent studies proposed new design requirements to mitigate column instability and brace failure through improved distribution of yielding along the height of the frame [8]. Additional research examined the contribution of adjacent gravity columns to the lateral load-resisting capacity of MT-CBFs, concluding that such interaction positively affects seismic performance [9]. A lateral design methodology was also introduced for single-tier concentrically braced frames, incorporating the combined effects of axial forces and in-plane moments in columns. This method addresses the issue of asymmetric plastic deformations in braces across the frame height, reducing drift concentration and enhancing overall nonlinear behavior. It was further observed that increasing seismic design forces alone does not significantly improve column moment stability or prevent buckling. However, considering fixed-base conditions in the design greatly enhances column response and prevents instability [10].

Research on MT-EBFs remains limited. The first numerical study used OpenSees to analyze the seismic behavior of a 9 meters tall, 7 meters span MT-EBF with various lateral bracing configurations for intermediate beams. In the first configuration, the intermediate beams were laterally braced, yielding satisfactory structural performance. In the second configuration, which lacked lateral bracing for intermediate beams, lateral-torsional buckling of the link was observed at a story drift ratio of 0.95%, indicating inadequate seismic performance [11]. Subsequent research proposed seismic analysis methodologies and design criteria to enhance the stability of two-tier MT-EBFs with I-shaped link beams. These recommendations included requirements for strength, stiffness, and stability of braces, inter-tier beams, and columns, aiming to: (1) limit excessive out-of-plane deformations, (2) facilitate sequential yielding in link beams, and (3) restrict inelastic link rotation in the tier with maximum lateral displacement [12]. Another investigation focused on lateral-torsional buckling in intermediate beams of MT-EBFs, evaluating four configurations of MT-EBFs with one or two intermediate tiers and two types of brace-to-beam connections. In the first configuration, braces were connected via gusset plates to the beam, while in the second, braces were directly welded to the beam using full-penetration welds. Results showed that lateral-torsional buckling occurred in intermediate beams with gusset plate connections due to insufficient stiffness. However, direct brace-to-beam connections provided adequate stiffness, preventing buckling in intermediate beams [13]. Although the research of the experimental study consisted of testing of six nearly full-scale EBFs where the test results demonstrated that short links with link length ratios less than 1.22 can experience inelastic link rotations greater than the codified limit of 0.08 rad even without lateral bracing. The numerical results showed that I-shaped links without lateral bracing can provide a stable response when the link length ratio is less than 1.15. In addition to this limit, the ratio of the elastic critical buckling capacity to the plastic shear capacity should be greater than 3.5 and 2.5 for links with and without axial force, respectively [14].

This study aims to compare the buckling behavior of intermediate link connected to diagonal braces through gusset plates in 4-Tiered Eccentrically Braced Frame (4T-EBF) using I-shaped and box sections. Previous investigations have confirmed that direct connections between braces and beams can effectively mitigate buckling in intermediate link [13]. In this research, two 4T-EBF configurations incorporating both I-shaped and box link is examined using advanced numerical modeling in Abaqus. Due to the absence of specific seismic design provisions for MT-EBFs, the design process adheres to the guidelines established for conventional EBF. Notably, the link beams located in the intermediate tiers are modeled without lateral bracing, reflecting practical constraints commonly encountered in real-world construction. Following the member design phase, comprehensive three-dimensional finite element models are developed in Abaqus. The

structural performance is then evaluated through nonlinear static (pushover) analyses, with the target maximum inter-story drift ratio set at 3%.

2- SEISMIC DESIGN BASED ON AISC 341-22

A single-story industrial steel building located in San Francisco, California, was selected as the case study. The building has a plan dimension of 56 × 63 meters, with a uniform bay spacing of 7 meters in all directions and an overall height of 12 meters, consisting of three intermediate tiers. In each of the two principal directions, a multi-tier eccentrically braced frame (MT-EBF) is implemented. The braces are connected to the beams via gusset plates. The link is modeled using rolled wide-flange (W-shaped) I-sections and the box section is fabricated from steel plates. A link length (e) of 0.7 meters is adopted to ensure shear behavior. The roof of the structure is subjected to a uniformly distributed dead load and live load of 1.0 kPa each, in addition to a snow load of 0.35 kPa. An exterior wall load of 1.0 kPa is also considered in the design. In the absence of dedicated seismic design provisions for MT-EBFs, the seismic design criteria were adopted based on the provisions for conventional eccentrically braced frames (EBFs) as specified in ASCE 7-22. The system design employs a response modification coefficient of R=8, a deflection amplification factor of C_d=4 and an overstrength factor of Ω_0=2. An importance factor of I_e=1.0 is also utilized. The structure is assumed to be located on Site Class D in San Francisco, California, and is designed based on the site-specific spectral acceleration parameters S_{DS}=1.16g and S_{D1}=1.17g, leading to a computed seismic response coefficient of C_s=0.145. Furthermore, all MT-EBF structural members are designed and checked for the combined demands imposed by seismic, gravitational, and wind loading conditions in compliance with relevant design standards.

The design of the link was carried out in accordance with the provisions of AISC 341-22, utilizing the seismic load combinations specified in ASCE 7-22. I-shaped link fabricated from ASTM A992 Grade 50 steel and ASTM A572 Grade 50 for box link were employed, characterized by a specified yield strength of F_y=345 Mpa and an expected yield strength of R_yF_y=380 MPa. To ensure a shear yielding mechanism, the link length (e) was restricted to a maximum of $1.6M_p/V_p$, where M_p and V_p represent the plastic moment and plastic shear capacity of the link, respectively. A link length of e=0.7 m was adopted. Moreover, the web and flange thickness of the link was designed to satisfy the slenderness requirements for highly ductile members, as defined by the λ_{hd} criterion. To determine the internal forces in members located outside the link portion, the maximum shear forces developed in the link were calculated. The expected shear and moment demand on the link were evaluated based on the capacity-limited earthquake force of the link. Accordingly, the expected shear force and flexural moment are defined as $V_{Ecl}=1.25R_yV_p$ and $M_{Ecl}=1.25RyV_pe/2$ for the I-shaped section, and as $V_{Ecl}=1.4R_yV_p$ and $M_{Ecl}=1.4RyV_pe/2$ for the box, as illustrated in Figure 2 [15].

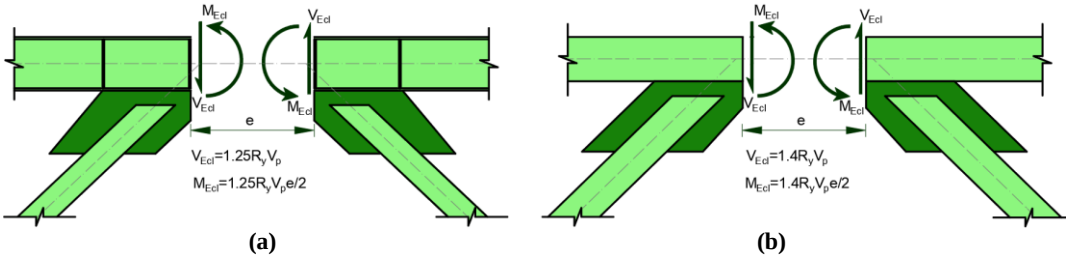

Figure 2- The expected shear and flexural moment in the link based on the capacity-limited earthquake force (a) I-shaped Link (b) Box link

The beams outside the link portion were designed as continuous members, utilizing the same cross-sectional shape and dimensions as the link. According to AISC 341-22, for beams with floor slabs beyond the link portion, an expected shear force of $0.88\times V_{Ecl}$ may be used, omitting the R_y factor. However, in MT-EBF systems where intermediate-tier link lack floor slabs, the expected shear force was estimated using the V_{Ecl}. These beams were designed as beam-columns to resist the combined effects of weak-axis axial forces and strong-axis flexural moments resulting from gravity loads, as well as moments induced by the maximum shear forces generated in the link. The braces were constructed using hollow structural sections (HSS) fabricated from ASTM A500 Grade B42 steel with a yield stress of F_y=290MPa. These sections were selected due to their high efficiency and equal radius of gyration about both principal axes. Columns were designed as continuous members throughout the full height of the frame and were composed of wide-flange I-shaped sections made of ASTM A992 Grade 50 steel with a yield stress of F_y=345MPa. Column orientations were chosen such that their strong axis is perpendicular to the plane of the frame. The column design forces were determined in accordance with AISC 341-22 through two analyses. In the first analysis, column forces were obtained based

on capacity-limited earthquake force (E_{cl}), derived using capacity-based analysis of the link beams. The second analysis incorporated the overstrength seismic load, in which the seismic forces were increased by applying the overstrength factor (Ω_o). These overstrength forces were considered exclusively for assessing axial loads in the columns, while flexural moments were disregarded during this evaluation. According to ASCE 7 provisions, the story drift MT-EBFs with Risk Category III must be limited to a maximum of 2% of the story height. The design of link stiffeners was based on their shear behavior and the expected link rotation angle. Each pair of stiffeners was installed on both sides of the web along its full height. Gusset plates were designed to transfer axial forces from braces to the beam-column joints, in compliance with AISC 360-22 and AISC 341-22 provisions. The primary objectives in designing the gusset plates were to ensure sufficient strength, prevent yielding or buckling, and maintain elastic behavior under seismic loading. The geometric configuration, positioning, and connection layout of the gusset plates were determined using the Uniform Force Method (UFM) recommended by AISC. The final design outcome of the four-tier eccentrically braced frame (EBF) is illustrated in Figure 3.

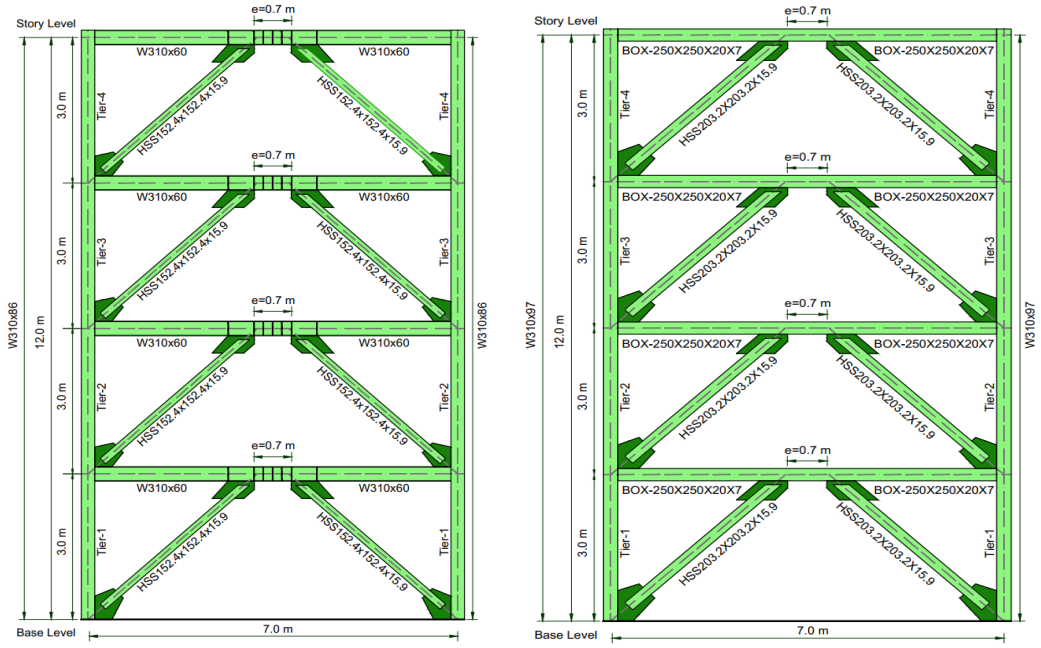

(a) **(b)**

Figure 3- The design results of the 4T-EBF frame members (a) with I-shaped link (b) with box link

3- NUMERICAL SIMULATION AND VERIFICATION

Before modeling the MT-EBF frames, it was necessary to validate the nonlinear behavior of steel material, the modeling procedure in Abaqus, and the buckling behavior of beam members. These verifications were conducted to ensure accurate representation of member limit states and to reliably predict nonlinear behavior and the onset of buckling. A three-dimensional finite element model was developed, incorporating the nonlinear material behavior using four-node shell elements (S4R) capable of simulating 3D deformations. To simulate pinned boundary conditions, the base of the columns and the bottom edge of the gusset plates were released in rotational degrees of freedom (UR1 and UR3), allowing rotation in and out of the frame plane. The top-tier beams in all frames were restrained against in-plane displacements at the top and bottom flanges to simulate lateral bracing at the roof level. The elastic behavior of steel was modeled with a Young's modulus of $E = 2\times10^5$ MPa and a Poisson's ratio of $\nu = 0.3$. Given the expected inelastic deformation demands during seismic loading, MT-EBFs members are anticipated to undergo significant yielding and large plastic deformations. Therefore, a material model capable of simulating the cyclic inelastic behavior of steel, including both isotropic and kinematic hardening, was required. The combined kinematic/isotropic hardening plasticity model from the Abaqus material library was employed to simulate the cyclic plastic response of steel [16].

The cyclic plastic response was simulated using the Voce-Chaboche constitutive model, calibrated through experimental data for both isotropic and kinematic hardening parameters. The calibration was based on experimental results from shear link fabricated from wide-flange sections, selected to represent the prototype frame [17]. A W10×33 section with a length of 584 mm was modeled and subjected to boundary

conditions replicating the laboratory setup, under the displacement-controlled loading protocol specified by AISC 2002. For the box link model, a beam with a box section was used, featuring a flange width of 152 mm and thickness of 16 mm, a web height of 152 mm and thickness of 8 mm, and a total length of 456 mm [18]. To ensure modeling accuracy, a mesh size of 25 mm was employed for the finite element analysis. Parameters defining the combined hardening behavior of steel materials in the Abaqus model were derived from calibration and must be obtained from laboratory test results. In the Abaqus model, three parameters define the kinematic/isotropic material model: the yield stress at zero strain (F_y), the initial kinematic hardening (C_1), and the rate of softening (γ). Each of these parameters was calibrated through the validation process, the simulation results demonstrated excellent agreement with the experimental data. The accuracy of the modeling was confirmed through the hysteresis response, which is illustrated in Figure 4. Moreover, to enhance the precision of the model, buckling analysis was conducted to determine the critical buckling modes. The applied geometric imperfection was assumed as 1/200 of the unbraced length of the members.

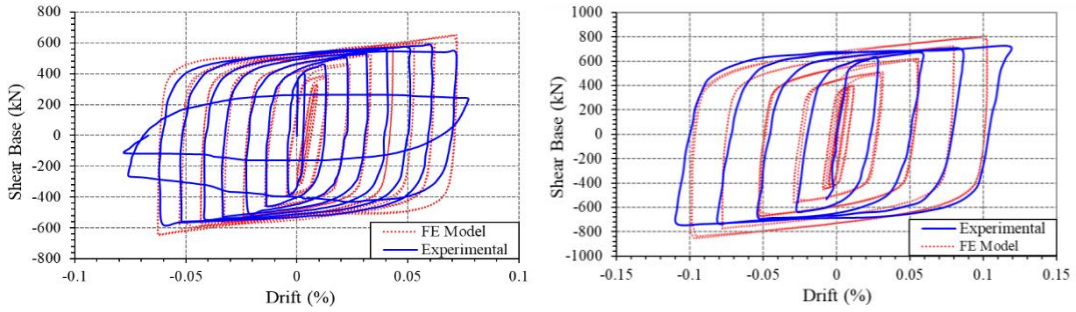

(a) **(b)**

Figure 4- Numerical validation and comparison of FE modeled and laboratory hysteresis curves (a) for I-shaped link (b) for box link

To ensure accurate prediction of the lateral-torsional buckling onset in the intermediate beams of the MT-EBF tiers, a validation study was conducted using a simply supported beam with a length of 6000 mm, a web height of 500 mm and thickness of 8 mm, and flange width of 200 mm with a thickness of 16 mm [19]. The beam was fabricated from S460NL structural steel, with a reported yield strength of F_y = 522 MPa and an ultimate strength of F_u = 656 MPa. An initial geometric imperfection equivalent to 1/200 of the unbraced length was introduced to represent fabrication tolerances. The beam was subjected to loading at two locations spaced 1015 mm apart near the beam ends. A comparison of the numerical and experimental results for the vertical displacement under axial loading is presented in Figure 5a, demonstrating good agreement and validating the model's ability to capture the onset of lateral-torsional buckling. To ensure the accurate prediction of buckling onset in the columns of the MT-EBF frame, a validation study was conducted on a column specimen with a length of 3725 mm and a W310×129 section made of ASTM A992 Grade 50 steel, having a yield strength of F_y = 345 MPa [20]. An initial imperfection equivalent to 1/200 of the unbraced length was introduced to simulate fabrication imperfections. A comparison between the numerical and experimental results for the axial load versus vertical displacement at the loading point is presented in Figure 5b. Nonlinear static (pushover) analysis was conducted by applying a monotonically increasing lateral in-plane displacement at the top ends of the braced frame columns until the target drift reached 3% of the structure's height [21].

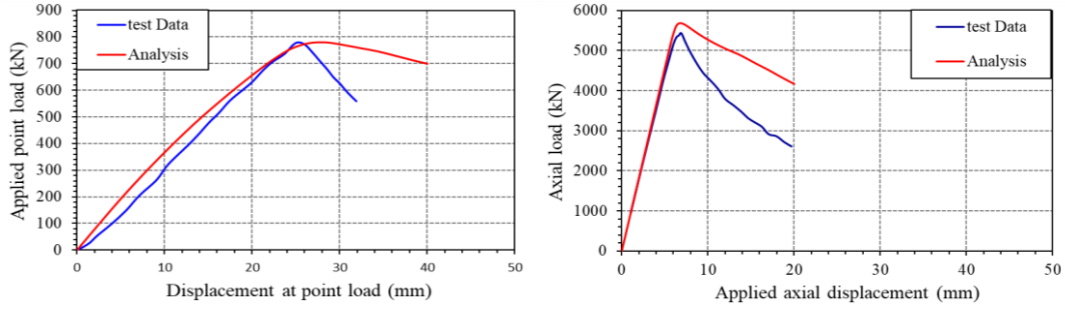

(a) **(b)**

Figure 5- (a) Comparison of modeled and experimental FE hysteresis curves for lateral-torsional buckling of a beam (b) Comparison of modeled and experimental FE hysteresis curves for column buckling

4- FINDINGS FROM THE NONLINEAR STATIC ANALYSIS

The overall seismic response of the frames, including the capacity curves, link rotations, and the internal forces developed in structural members such as link and columns, is discussed.

The outcomes of the nonlinear static (pushover) analysis for the MT-EBF frame with four braced tiers with I-shaped link are presented in Figure 6. Figure 6a displays the stress contours and deformation patterns at a 3% story drift, revealing localized stress concentrations and the overall deformation mechanism. As shown in the capacity curve in Figure 6b, the structure experiences a loss of global stability at a relatively small drift of 0.2%, indicating inadequate lateral performance and limited deformation capacity. The evolution of link rotation with respect to story drift is illustrated in Figure 6c. The fourth-tier link, which benefits from effective lateral bracing, exhibits stable inelastic rotational behavior throughout the drift range. In contrast, the first-tier link undergoes lateral-torsional buckling shortly after yielding and becomes unstable at a drift of 0.3%. The second-tier link demonstrates intermediate behavior, losing stability at 2.3% drift, while the third-tier link buckles at 2.8%, highlighting a progressive degradation of performance in unbraced tiers. Figure 6d depicts the variation of shear force in the link as a function of story drift. The fourth-tier link maintains consistent shear strength with increasing drift, while the first-tier link exhibits a substantial drop in shear force at 0.3% drift, aligning with the onset of lateral-torsional buckling. The second- and third-tier links also experience shear degradation at drifts of 2.3% and 2.8%, respectively, confirming their limited ability to sustain inelastic demand without bracing. Figure 6e shows the relationship between shear force and link rotation. All links exhibit nonlinear behavior beginning at approximately 0.01 radians of rotation. The fourth-tier link continues to resist shear effectively, but the links in the first through third tiers lose load-bearing capacity at rotations of 0.015, 0.16, and 0.19 radians, respectively. Notably, the first-tier link fails prior to reaching the code-defined drift limit, indicating its higher susceptibility to premature instability. Meanwhile, the second- and third-tier links exceed the allowable drift before experiencing failure, emphasizing the critical role of lateral bracing in ensuring link stability. Figure 6f presents the axial compressive force in the columns versus story drift. The expected axial demand based on the capacity-limited seismic force (E_{cl}) is approximately 1775 kN, while the force calculated using the overstrength factor (Ω_o) is about 1650 kN. Although the column was designed for the higher E_{cl} demand, the maximum axial force developed in the simulation is only 1450 kN—significantly lower than the expected design force. This suggests that the structural system becomes unstable and loses lateral load resistance before the design-level axial demand can develop. Lastly, Figure 6g shows the in-plane flexural moment in the column with respect to story drift. The peak moment is around 20 kN.m, notably exceeding the 6 kN.m predicted from linear analysis. Additionally, the moment estimated from the linear model at maximum drift is considerably lower than the actual demand, confirming that linear elastic analysis underestimates both drift and in-plane flexural demands. These findings underscore the importance of nonlinear analysis for accurately capturing the inelastic seismic behavior and failure modes of MT-EBF.

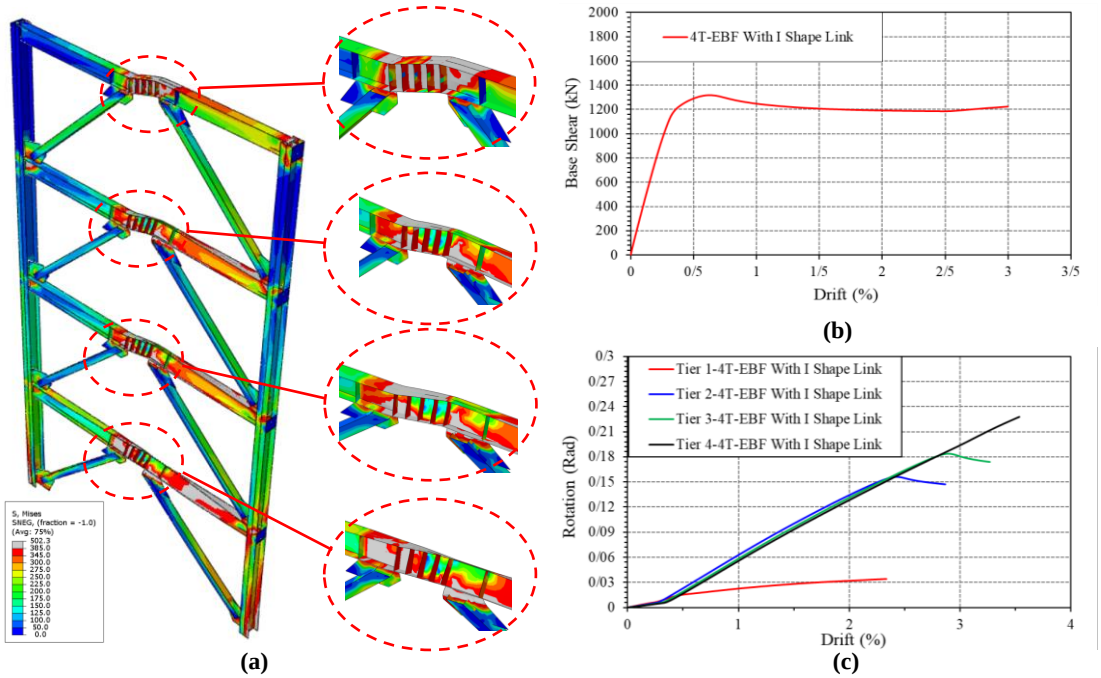

(a) (b) (c)

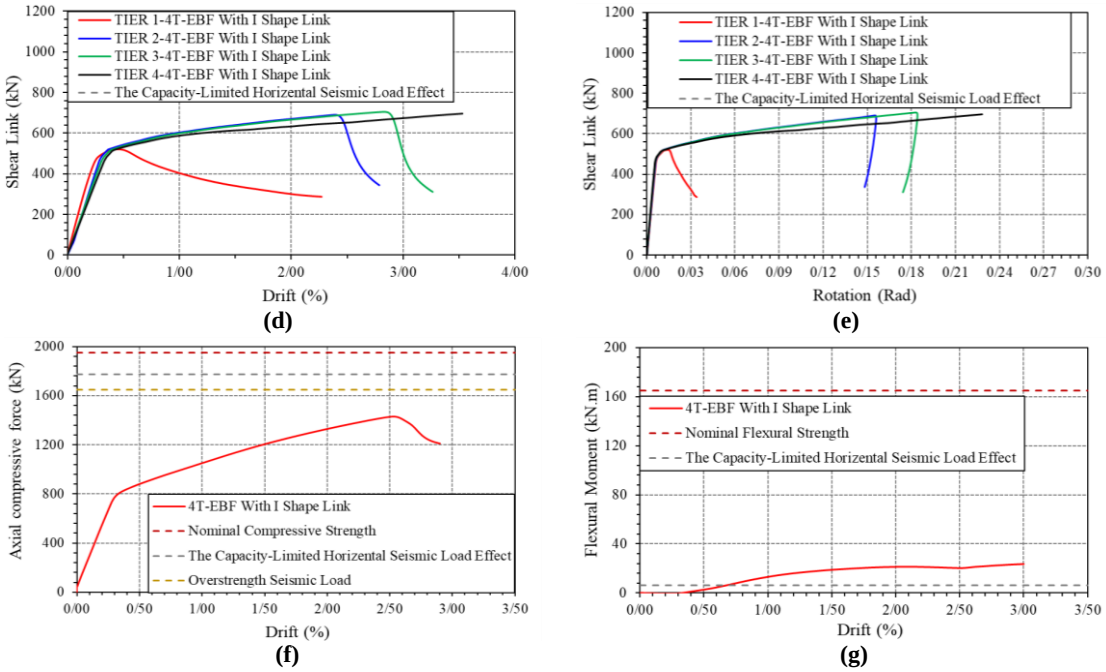

Figure 6- The diagrams obtained from the nonlinear static analysis for 4T-EBF frame with an I-shaped link (a) deformation and stress contour at drift of 3% (b) capacity curve (c) link rotation to drift ratio (d) drift to shear link curve (e) link rotation to shear link beam curve (f) drift to the axial compressive force curve (g) drift to in-plane flexural moment curve

In the MT-EBF configuration featuring four braced tiers and box links, the results of nonlinear static analysis indicate that all tiers initially participated in resisting lateral seismic loads. Despite the absence of lateral bracing in the intermediate tiers, no lateral-torsional buckling was observed in any of the link. Instead, the compression column exhibited out-of-plane buckling due to axial compressive forces. The results of the pushover analysis are summarized in Figure 7. Figure 7a illustrates the stress contours and deformation of the four-tier MT-EBF frame, highlighting the regions of localized plasticity and structural instability. According to the capacity curve depicted in Figure 7b, the structure experienced compression induced buckling of the column at a drift level of 2.1%, signifying the onset of global instability and an inability to sustain further lateral deformation. The drift-link rotation relationship shown in Figure 7c reveals that none of the links maintained stable rotational behavior throughout the loading process. The first-tier link failed prematurely at a drift of 1.5%, while the links in the second to fourth tiers exhibited progressive degradation and ceased rotation at a drift of approximately 2.5%. Figure 7d displays the variation of link shear force as a function of story drift. All links initially exhibited stable shear behavior, with lateral load resistance increasing alongside the applied drift. However, following the buckling of the compression column in the first tier, the corresponding link lost its load-bearing capacity earlier than the others, failing at a drift of 1.5%. The remaining links in tiers two through four ultimately failed at a drift of 2.5%, correlating with a decline in their shear strength and energy dissipation capacity. Figure 7e presents the relationship between link shear force and rotation. All links entered the nonlinear deformation range at approximately 0.01 radians and initially demonstrated stable shear responses with increasing rotation. Nevertheless, shear instability developed at rotation values of 0.09, 0.15, 0.15, and 0.13 radians for the first through fourth tiers, respectively. These rotations correspond to the point of peak shear resistance, beyond which the links experienced a reduction in lateral strength. Notably, the linear analysis underestimated the maximum shear demand in all tiers. At drift ratios of 0.363%, 0.449%, 0.510%, and 0.551% for the first to fourth tiers, respectively, the predicted shear forces were lower than the actual demands observed in the nonlinear analysis. In contrast, at the design drift limit of 2%, the actual shear force exceeded the expected value by approximately 20%, indicating that linear procedures are unconservative in estimating link demand. Similarly, the rotations derived from linear analysis—0.0272, 0.0337, 0.0382, and 0.0413 radians—were significantly lower than the actual rotations associated with peak shear strength. At the code-defined allowable rotation of 0.08 radians, the actual shear forces were markedly higher than predicted, emphasizing the importance of nonlinear analysis for accurate link design. The variation of axial compressive force in the column relative to story drift is presented in Figure 7f. The column experienced out-of-plane buckling at a drift of 2.4%, despite being designed for a capacity-limited seismic demand. A W360×122 section with a compressive capacity of 3150 kN was selected for this column. The expected axial force demand was 2800 kN, yet the maximum axial force developed during the analysis was only 2200 kN. At both the maximum

drift level predicted by linear analysis (0.551%) and the allowable drift of 2%, the actual axial force remained below the expected value. This indicates that the axial demand estimated through linear design procedures did not fully materialize, primarily because the system lost its lateral load-carrying capacity before reaching this level of axial compression. Lastly, Figure 7g illustrates the in-plane flexural moment in the column as a function of story drift. The peak in-plane moment reached approximately 50 kN·m, substantially exceeding the 17 kN·m predicted by linear analysis. However, at both the maximum drift obtained from the linear model and the allowable drift, the actual in-plane moments remained below the expected design demand. This result highlights the limitations of linear analysis in predicting inelastic behavior and confirms that nonlinear modeling is essential for capturing the full extent of column flexural demands under seismic loading.

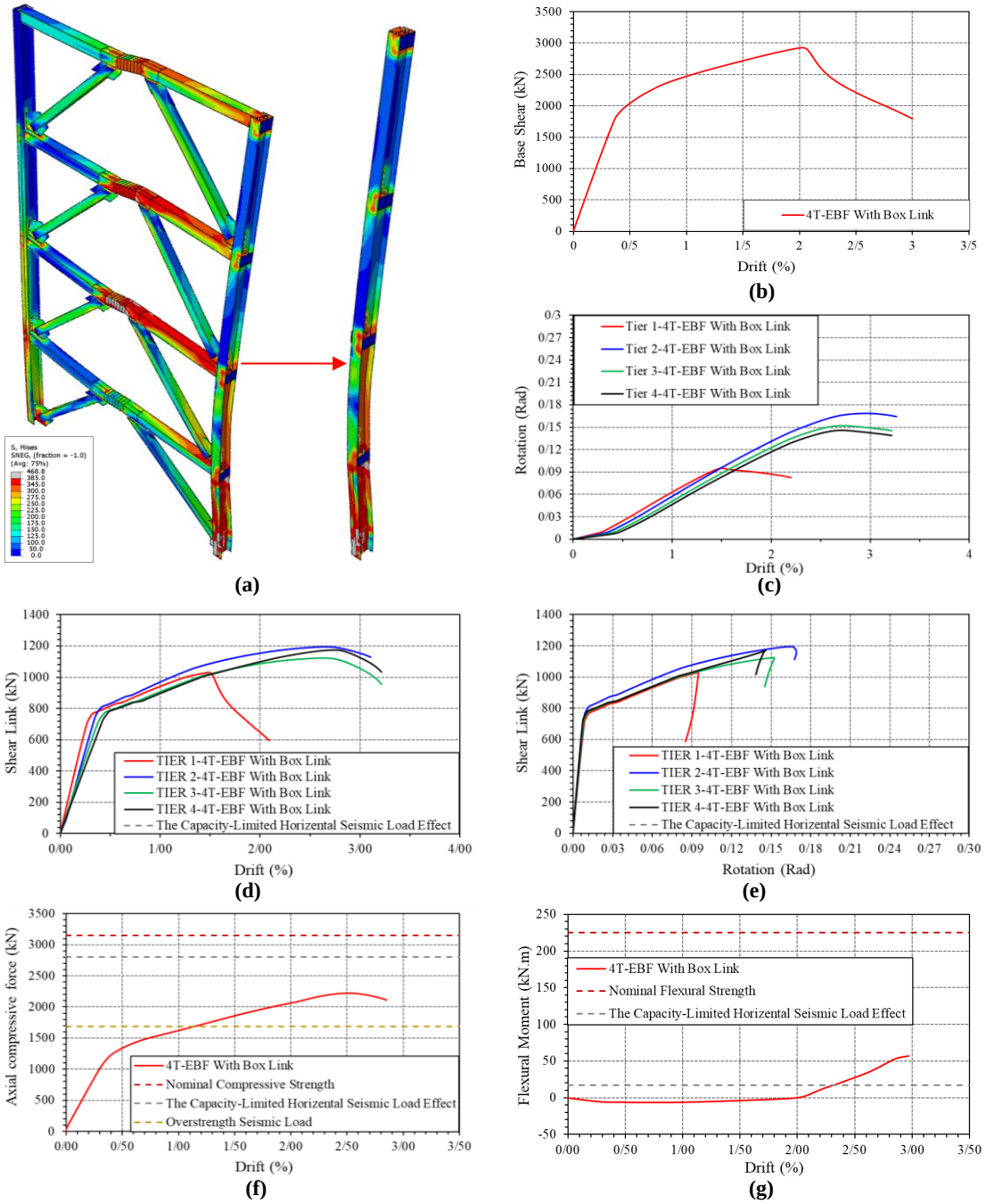

Figure 6- The diagrams obtained from the nonlinear static analysis for 4T-EBF frame with an box link (a) deformation and stress contour at drift of 3% (b) capacity curve (c) link rotation to drift ratio (d) drift to shear link curve (e) link rotation to shear link beam curve (f) drift to the axial compressive force curve (g) drift to in-plane flexural moment curve

5- CONCLUSIONS

This study investigated the seismic performance of multi-tier eccentrically braced frames (MT-EBFs) through detailed numerical modeling and nonlinear static analysis using Abaqus, in accordance with the seismic provisions of ANSI/AISC 341-22. The numerical models incorporated I-shaped link in a four-tier configuration with divergent bracing. To validate the accuracy of the simulations, the numerical results were compared against available experimental data. Additionally, the lateral-torsional buckling of link and flexural buckling of columns were calibrated based on experimental observations.

The results revealed that I-shaped links in unbraced intermediate tiers experienced lateral-torsional buckling, leading to a sudden reduction in lateral stiffness and localized instability. In contrast, box links showed no signs of lateral-torsional buckling even in the absence of lateral bracing; however, the MT-EBF configuration with box links columns exhibited column buckling induced by flexural demands significantly exceeding those predicted by linear analysis. Furthermore, the shear force demand in the link regions surpassed the nominal strength calculated expression in AISC 341-22, with increases of approximately 15% for I-shaped links and 20% for box links. This substantial increase indicates that the default overstrength factors in the current code may underestimate the actual shear demands in multi-tiered configurations.

The findings also revealed that the flexural moments in the columns increased by a factor of three to four compared to linear predictions, whereas axial force demands remained consistent with linear design values. This discrepancy highlights the inability of linear analysis to accurately capture the nonlinear flexural demands in columns, potentially leading to unexpected column instability or failure.

Overall, the results underscore the limitations of linear analysis in capturing the complex inelastic behavior and failure mechanisms of MT-EBFs. In multi-tier systems, the seismic response is influenced by the interaction of various buckling modes, redistribution of inelastic forces, and the critical role of lateral bracing for link stability. These complexities suggest that current code provisions alone may be insufficient for ensuring the safe and economical design of such systems. Therefore, further comprehensive studies are essential to develop refined design criteria based on nonlinear analysis and experimental evidence. These new provisions should specifically address the behavior of intermediate-tier link beams and the force transfer mechanisms to adjacent members, enabling more accurate estimation of structural demands under severe seismic events.

6- REFERENCES

[1] M. D. Engelhardt and E. P. Popov, “BEHAVIOR OF LONG LINKS IN ECCENTRICALLY BRACED FRAMES by,” 1989.

[2] A. Asghari and S. Saharkhizan, “Seismic design and performance evaluation of steel frames with knee-element connections,” *J Constr Steel Res*, vol. 154, pp. 161–176, 2019, doi: https://doi.org/10.1016/j.jcsr.2018.11.011.

[3] P. A. Cano, A. Imanpour, and A. Professor, “Evaluation of AISC Seismic Design Methods for Steel Multi-Tiered Special Concentrically Braced Frames.”

[4] K. D. Hjelmstad and E. P. Popov, “SEISMIC BEHAVIOR OF ACTIVE BEAM LINKS IN ECCENTRICAllY BRACED FRAMES NATIONAL TECHNICAL INfORMATION SERVICE,” 1983.

[5] M. Bani and A. Imanpour, “Seismic Performance Assessment of Multitiered Steel Buckling-Restrained Braced Frames Designed to 2010 and 2022 AISC Seismic Provisions,” *Journal of Structural Engineering*, vol. 150, no. 9, p. 4024113, 2024, doi: 10.1061/JSENDH.STENG-13327.

[6] P. A. Cano and A. Imanpour, “Evaluation of Seismic Design Methods for Steel Multi-Tiered Special Concentrically Braced Frames.”

[7] A. Imanpour, C. Stoakes, R. Tremblay, L. Fahnestock, and A. Davaran, “Seismic Stability Response of Columns in Multi-Tiered Braced Steel Frames for Industrial Applications,” 2013.

[8] A. Imanpour and R. Tremblay, “Seismic design and response of steel multi-tiered concentrically braced frames in Canada,” *Canadian Journal of Civil Engineering*, vol. 43, no. 10, pp. 908–919, 2016, doi: 10.1139/cjce-2015-0399.

[9] A. Imanpour, K. Auger, and R. Tremblay, “Seismic design and performance of multi-tiered steel braced frames including the contribution from gravity columns under in-plane seismic demand,” *Advances in Engineering Software*, vol. 101, pp. 106–122, 2016, doi: https://doi.org/10.1016/j.advengsoft.2016.01.021.

[10] C. D. Stoakes and L. A. Fahnestock, "Strong-Axis Stability of Wide Flange Steel Columns in the Presence of Weak-Axis Flexure," *Journal of Structural Engineering*, vol. 142, no. 5, p. 4016004, 2016, doi: 10.1061/(ASCE)ST.1943-541X.0001448.

[11] A. Ashrafi and A. Imanpour, "Seismic response of steel multi-tiered eccentrically braced frames," *J Constr Steel Res*, vol. 181, p. 106600, 2021, doi: https://doi.org/10.1016/j.jcsr.2021.106600.

[12] A. Ashrafi and A. Imanpour, "Analysis and Design Methods for Improved Stability of Two-Tiered Steel Eccentrically Braced Frames with Continuous I-Shaped Links," *Journal of Structural Engineering*, vol. 150, no. 9, p. 4024112, 2024, doi: 10.1061/JSENDH.STENG-12940.

[13] M. Rezaee and A. Asghari, "Lateral-torsional buckling investigation of multi-tiers eccentrically braced frames with shear link beam," *Structures*, vol. 68, p. 107063, 2024, doi: https://doi.org/10.1016/j.istruc.2024.107063.

[14] G. Yiğitsoy, C. Topkaya, and T. Okazaki, "Stability of beams in steel eccentrically braced frames," *J Constr Steel Res*, vol. 96, pp. 14–25, May 2014, doi: 10.1016/j.jcsr.2014.01.002.

[15] M. S. Speicher and J. L. Harris, "Collapse Prevention seismic performance assessment of new eccentrically braced frames using ASCE 41," *Eng Struct*, vol. 117, pp. 344–357, Jun. 2016, doi: 10.1016/j.engstruct.2016.02.018.

[16] J. L. Chaboche, "On some modifications of kinematic hardening to improve the description of ratchetting effects," *Int J Plast*, vol. 7, no. 7, pp. 661–678, 1991, doi: https://doi.org/10.1016/0749-6419(91)90050-9.

[17] T. Okazaki and M. D. Engelhardt, "Cyclic loading behavior of EBF links constructed of ASTM A992 steel," *J Constr Steel Res*, vol. 63, no. 6, pp. 751–765, 2007, doi: https://doi.org/10.1016/j.jcsr.2006.08.004.

[18] J. W. Berman and M. Bruneau, "Experimental and analytical investigation of tubular links for eccentrically braced frames," *Eng Struct*, vol. 29, no. 8, pp. 1929–1938, 2007, doi: https://doi.org/10.1016/j.engstruct.2006.10.012.

[19] T. Tankova, F. Rodrigues, C. Leitão, C. Martins, and L. Simões da Silva, "Lateral-torsional buckling of high strength steel beams: Experimental resistance," *Thin-Walled Structures*, vol. 164, p. 107913, 2021, doi: https://doi.org/10.1016/j.tws.2021.107913.

[20] C.-P. Lamarche and R. Tremblay, "Seismically induced cyclic buckling of steel columns including residual-stress and strain-rate effects," *J Constr Steel Res*, vol. 67, no. 9, pp. 1401–1410, 2011, doi: https://doi.org/10.1016/j.jcsr.2010.10.008.

[21] M. Esmaelian, S. Raza, M. Shekarchi, M. Motavalli, and M. Shahverdi, "Self-Centering of RC Columns with Prestressed Fe-SMA Reinforcement," *Procedia Structural Integrity*, vol. 64, pp. 2091–2100, 2024, doi: https://doi.org/10.1016/j.prostr.2024.09.306.